

# Learning Across Tasks and Domains

Pierluigi Zama Ramirez, Alessio Tonioni, Samuele Salti, Luigi di Stefano  
Department of Computer Science and Engineering (DISI)  
University of Bologna, Italy

{pierluigi.zama, alessio.tonioni, samuele.salti, luigi.distefano}@unibo.it

## Abstract

Recent works have proven that many relevant visual tasks are closely related one to another. Yet, this connection is seldom deployed in practice due to the lack of practical methodologies to transfer learned concepts across different trains. In this work, we introduce a novel adaptation framework that can operate across both task and domains. Our framework learns how to transfer knowledge across tasks in a completely supervised domain (e.g., synthetic data) and use this knowledge on a different domain where we have only partial supervision (e.g., real data). Our proposal is complementary to existing domain adaptation techniques and extends them to cross tasks scenarios providing additional performance gains. We prove the effectiveness of our framework across two challenging tasks (i.e., monocular depth estimation and semantic segmentation) and four different domains (Synthia, Carla, Kitty, and Cityscapes).

## 1. Introduction

Deep learning has revolutionized computer vision research and set forth a general framework to address a variety of visual tasks (e.g., classification, depth estimation, semantic segmentation, ...). The existence of a common framework suggests a close relationship between different tasks that should be exploitable to alleviate the dependence on huge labeled training sets. Unfortunately, most state-of-the-art methods ignore these connections and instead focus on a single task by solving it in isolation through supervised learning on a specific domain (i.e., dataset). Should the domain or task change, common practice would require the acquisition of a new annotated training set followed by retraining or fine-tuning the model. However, any deep learning practitioner can testify that the effort to annotate a dataset is usually quite substantial and does vary significantly across tasks, potentially requiring ad-hoc acquisition modalities. The question we try to answer is: *would it be possible to deploy the relationships between tasks to remove*

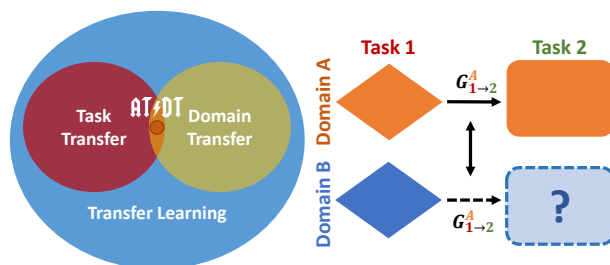


Figure 1: Our AT/DT framework transfers knowledge across tasks and domains. Given two tasks (1 and 2) and two domains (A and B), with supervision for both tasks in A but only for one task in B, we learn the dependency between tasks in A and exploit this knowledge in B to solve task 2 without the need of supervision.

*the dependence for labeled data on new domains?*

A partial answer to this question has been provided by [43], which formalizes the relationships between tasks within a specific domain into a graph referred to as *Taskonomy*. This knowledge can be used to improve performance within a fully supervised learning scenario, though it is not clear how well may it generalize to new domains and to which extent may it be deployed in a partially supervised scenario (i.e., supervision on only some tasks/domains). Generalization to new domains is addressed in the domain adaptation literature [38], that, however, works under the assumption of solving a single task in isolation, therefore ignoring potential benefits from related tasks.

We fuse the two worlds by explicitly addressing a cross domain and cross task problem where on one domain (e.g., synthetic data) we have annotations for many tasks, while in the other (e.g., real data) annotations are available only for a specific task, though we wish to solve many.

Purposely, we propose a new ‘Across Tasks and Domains Transfer framework’ (shortened AT/DT) which learns in a specific domain a function  $G_{1 \rightarrow 2}$  to transfer knowledge between a pair of tasks. After the training phase, we show that the same function can be applied in a new do-

main to solve the second task while relying on supervision only for the first. A schematic representation of AT/DT is pictured in Fig. 1.

We prove the effectiveness of AT/DT on a challenging autonomous driving scenario where we address the two related tasks of depth estimation and semantic segmentation [29]. Our framework allows the use of fully supervised synthetic datasets (*i.e.*, Synthia [17], and Carla [7]) to drastically boost performance on partially supervised real data (*i.e.*, Cityscapes [5] and Kitti [11, 27]). Finally, we will also show how AT/DT is robust to sub-optimal scenarios where we use only few annotated real samples or noisy supervision by proxy labels [23, 40, 34].

The novel contributions of this paper can be summarized as follows:

- To the best of our knowledge, we are the first to study a cross task and cross domain problem where we have supervision for all tasks in one domain while only for a subset of them in the other.
- We propose a general framework to address the aforementioned problem that learns to transfer knowledge across tasks and domains
- We show that it is possible to directly learn a mapping between representations suitable for different tasks and that this function generalizes well to unseen data both in the same domain as well as in new ones.

## 2. Related Work

**Transfer Learning:** The existence of related representation within CNNs trained for different tasks has been highlighted since early works in the field [41]. These early findings have motivated the use of transfer learning strategy to bootstrap learning across related tasks, *e.g.*, object detection networks are usually initialized with Imagenet weights [31, 16], even if [15] has recently challenged this paradigm. Luo et al. [26] fuse transfer learning strategy with domain adaptation technique to transfer representation across tasks and domains, however, their definition of tasks corresponds to different sets of classes in a classification problem, while we consider any visual tasks. Recently Zamir et. al. [43] have tried to formalize and deploy the idea of reusing information across training by proposing a computational approach to find relationships among visual tasks encoded in a taxonomy. Pal et. al. [28], propose to use a similar relationship knowledge together with meta learning to learn how to perform a new task in a zero shot scenario. Both [43] and [28] assume a shared domain across the tasks being addressed, instead we directly target a cross domain scenario. Moreover, [43] assumes full supervision to be available for all tasks while [28] zero supervision for the target task, Our work instead leverages on complete supervision for all tasks

in a domain and only partial supervision in a different (target) domain.

**Multi-task Learning:** Multi-task learning tries to learn many tasks simultaneously to obtain more general models or multiple outputs in a single run [24, 6, 14]. Some recent works directly addressed the autonomous driving scenario [3, 29] by learning simultaneously related tasks like depth estimation and semantic segmentation in order to improve performance. Kendall et al. [4] additionally considers the instance segmentation task and show that it is possible to train a single network to solve the three tasks by fusing the different losses through uncertainty estimation. Our work, instead, directly targets a single task but tries to use the relationship between related tasks to alleviate the need for annotations.

**Domain Adaptation:** A recent survey of the domain adaptation literature can be found in [39]. The idea behind this field of work is to learn models robust when tested on data sampled from a domain different than the training one. Earliest approaches such as [12, 13] try to build intermediate representations across domains, while recent ones, specifically designed for deep learning, focus on adversarial training at either pixel or feature level. Pixel level methods [33, 46, 2, 30] try to transform input images from one domain to the other using recently proposed image-to-image translation GANs [47, 22]. Feature level methods, instead, [20, 25, 37, 36, 9, 44, 35] try to align the feature representation extracted from CNN across different datasets, again often by means of GANs. Finally, recent works [32, 19, 45] operate both at pixels and features level. All these works focus on a single specific task (usually semantic segmentation) whilst our framework leverages the information from different tasks. As such, our new formulation can be seen as complementary to existing domain adaptation techniques.

## 3. Across Task and Domain Transfer Framework

We wish to start with a practical example of the problem we are trying to solve and how we address it. Let us consider a synthetic and real domain where we aim to solve the semantic segmentation task. Annotations come for free in the synthetic domain while are rather expensive in the real one. Domain adaptation comes handy for this; however, we wish to go one step further. May we pick a closely related task (*e.g.*, depth estimation) where annotations are available in both domains and use it to boost the performance of semantic segmentation on real data? To achieve this goal we train deep networks for depth and semantic segmentation on the synthetic domain and learn a mapping function to transform deep features suitable for depth estimation into deep features suitable for semantic segmentation. Then we apply the same mapping function on samples from the real domain to obtain a semantic segmentation model without

the need of annotation. In the remainder of this section, we formalize the AT/DT framework.

### 3.1. Common Notation

We denote with  $\mathcal{T}_j$  a generic visual task defined as in [43]. Let's assume  $\mathcal{X}^k$  to be the set of samples (*i.e.*, images) belonging to domain  $k$  and  $\mathcal{Y}_j^k$  to be the paired set of annotations for task  $\mathcal{T}_j$ . In our problem we assume to have two domains,  $\mathcal{A}$  and  $\mathcal{B}$ , and two tasks,  $\mathcal{T}_1$  and  $\mathcal{T}_2$ . For the two tasks we have complete supervision in  $\mathcal{A}$ , *i.e.*,  $\mathcal{Y}_1^{\mathcal{A}}$  and  $\mathcal{Y}_2^{\mathcal{A}}$ , but labels only for  $\mathcal{T}_1$  in  $\mathcal{B}$ , *i.e.*  $\mathcal{Y}_1^{\mathcal{B}}$ . We assume each task  $\mathcal{T}_j$  to be solvable by a deep neural network  $N_j$ , composed of a feature encoder  $E_j$  and a feature decoder  $D_j$ , such that  $\hat{y}_j = N_j(x) = D_j(E_j(x))$ . The network is trained on the domain  $k$  by minimizing a task-specific loss on annotated samples  $(x^k, y_j^k) \sim (\mathcal{X}^k, \mathcal{Y}_j^k)$ . The result of this training is a network trained to solve  $\mathcal{T}_j$  using samples from  $\mathcal{X}^k$  that we denote with  $N_j^k$ .

### 3.2. Overview

Our work builds on the intuition that if two tasks are related it should exist a function  $G_{1 \rightarrow 2} : \mathcal{T}_1 \rightarrow \mathcal{T}_2$  that transfer knowledge among them. But what does transferring knowledge means? We will show that this abstract concept can be implemented by transferring representations in deep feature space. We propose to first train two task specific network  $N_1$  and  $N_2$ , then approximate function  $G_{1 \rightarrow 2}$  by a deep neural network that transforms features extracted by  $N_1$  into corresponding features extracted by  $N_2$  (*i.e.*,  $G_{1 \rightarrow 2} : E_1(x) \rightarrow E_2(x)$ ). We train  $G_{1 \rightarrow 2}$  by minimizing a reconstruction loss on  $\mathcal{A}$ , where we have complete supervision for both tasks, and use it on  $\mathcal{B}$  to solve  $\mathcal{T}_2$  having supervision only for  $\mathcal{T}_1$ .

Our method can be summarized by the four steps pictured in Fig. 2 and detailed in the following sections:

1. Learn to solve task  $\mathcal{T}_1$  on domains  $\mathcal{A}$  and  $\mathcal{B}$ .
2. Learn to solve task  $\mathcal{T}_2$  on domain  $\mathcal{A}$ .
3. Train  $G_{1 \rightarrow 2}$  on domain  $\mathcal{A}$ .
4. Apply  $G_{1 \rightarrow 2}$  to solve  $\mathcal{T}_2$  on domain  $\mathcal{B}$ .

### 3.3. Solve $\mathcal{T}_1$ on $\mathcal{A}$ and $\mathcal{B}$

A network  $N_1$  can be trained to solve task  $\mathcal{T}_1$  on domain  $\mathcal{X}^k$  by minimizing a task specific supervised loss

$$L_{\mathcal{T}_1}(\hat{y}_1^k, y_1^k); \hat{y}_1^k = N_1(x^k). \quad (1)$$

However, training one network for each domain would likely result in disjoint feature spaces; we, instead, wish to have similar representation to ease the generalization of  $G_{1 \rightarrow 2}$  across domains. Therefore, we train a single network,  $N_1^{A \cup B}$ , on samples from both domains, *i.e.*,  $\mathcal{X}^k = \mathcal{X}^A \cup \mathcal{X}^B$ . Having a common representation let us learn a

task transfer mapping valid on both domains even though training it only on  $\mathcal{A}$ . More details on the impact of having common or disjoint networks are reported in Sec. 6.2.

### 3.4. Solve $\mathcal{T}_2$ on $\mathcal{A}$

Now we wish to train a network to solve  $\mathcal{T}_2$ , however, for this task we can only rely on annotated samples from  $\mathcal{A}$ . The best we can do is to train a  $N_2^{\mathcal{A}}$  minimizing a supervised loss

$$L_{\mathcal{T}_2}(\hat{y}_2^{\mathcal{A}}, y_2^{\mathcal{A}}); \hat{y}_2^{\mathcal{A}} = N_2(x^{\mathcal{A}}). \quad (2)$$

### 3.5. Train $G_{1 \rightarrow 2}$ on $\mathcal{A}$

We are now ready to train a task transfer network  $G_{1 \rightarrow 2}$  that should learn to remap deep features suitable for  $\mathcal{T}_1$  into good representations suitable for  $\mathcal{T}_2$ . Given  $N_1^{A \cup B}$  and  $N_2^{\mathcal{A}}$  we generate a training set with pairs of features  $(E_1^{A \cup B}(x^{\mathcal{A}}), E_2(x^{\mathcal{A}}))$  obtained feeding the same input  $x^{\mathcal{A}}$  to  $N_1^{A \cup B}$  and  $N_2^{\mathcal{A}}$ . We use only samples from  $\mathcal{A}$  for the training set as it is the only domain where we are reasonably sure that the two networks perform well. We optimize the parameters of  $G_{1 \rightarrow 2}$  by minimizing the reconstruction error between transformed and target features

$$L_{Tr} = \|G_{1 \rightarrow 2}(E_1^{A \cup B}(x^{\mathcal{A}})) - E_2(x^{\mathcal{A}})\|_2, \quad (3)$$

At the end of the training  $G_{1 \rightarrow 2}$  should have learned how to remap one deep feature into the other.

Among all the possible splits  $(E, D)$  obtained from  $N$  cutting it at different layers, we use as input for  $G_{1 \rightarrow 2}$  the deepest features, *i.e.*, those at the lowest spatial resolution. We pick this  $E$  because deeper features are usually considered less connected to a specific domain and more correlated to higher level concepts. Therefore, by learning a mapping at this level we hope to suffer less from domain shift when applying  $G_{1 \rightarrow 2}$  on samples from  $\mathcal{B}$ . A more in depth discussion on the choice of  $E$  is reported in Sec. 6.1.

### 3.6. Apply $G_{1 \rightarrow 2}$ to solve $\mathcal{T}_2$ on $\mathcal{B}$

Now we have all the components we need to solve  $\mathcal{T}_2$  on  $\mathcal{B}$ . We can use the supervision provided for  $\mathcal{T}_1$  on  $\mathcal{B}$  to extract good image features (*i.e.*,  $E_1^{A \cup B}(x_B)$ ). Then use  $G_{1 \rightarrow 2}$  to transform these features into good features for  $\mathcal{T}_2$ , and finally decode them through a suitable decoder  $D_2^{\mathcal{A}}$ . The formalization of our system at inference time is:

$$\hat{y}_2^{\mathcal{B}} = D_2^{\mathcal{A}}(G_{1 \rightarrow 2}(E_1^{A \cup B}(x_B))) \quad (4)$$

Thanks to our novel formulation, supervision for a certain task can be used to solve another (related) task on a novel domain without the need of annotations for the target task and domain.

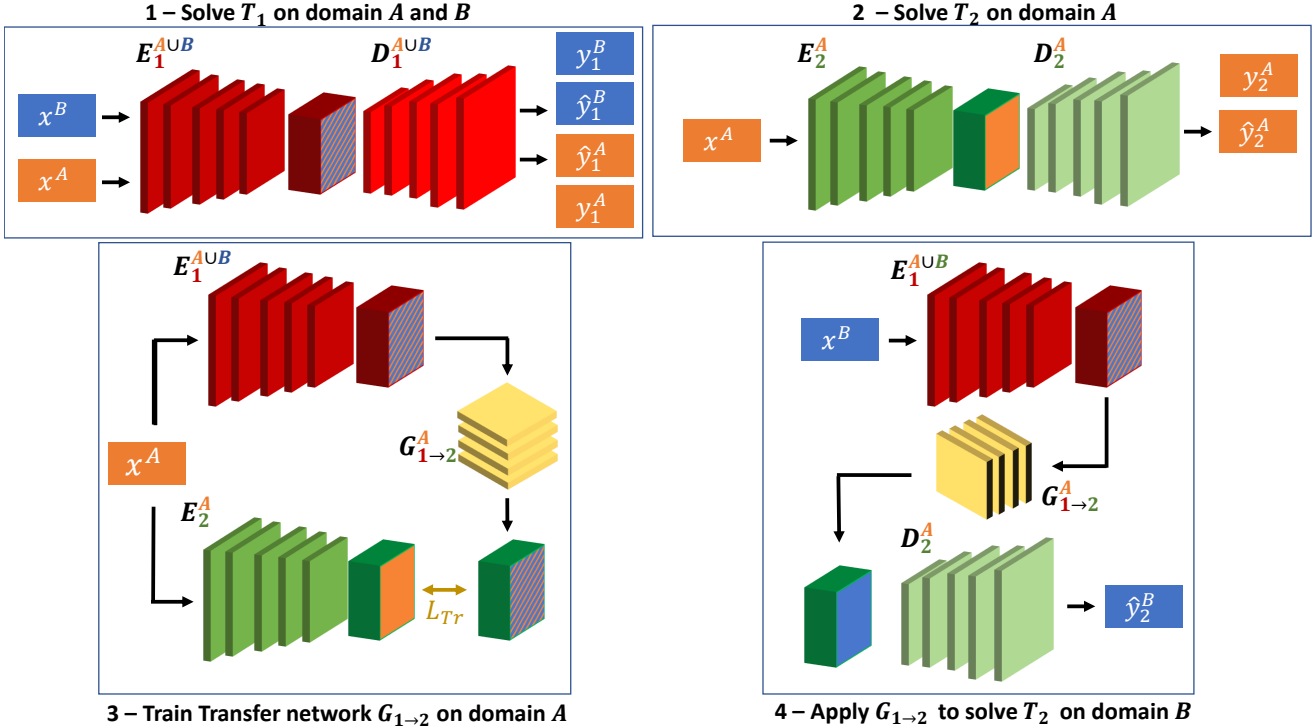


Figure 2: Overview of the AT/DT framework. We propose a four steps framework which allows to transfer knowledge across tasks and domains. (1) We train network  $N_1^{AUB}$  to solve  $\mathcal{T}_1$  (red) with supervision in domain  $\mathcal{A}$  (orange) and  $\mathcal{B}$  (blue) such that it should achieve a shared feature representation across domains, highlighted by blue and orange strips. (2) We train a network  $N_2^A$  to solve  $\mathcal{T}_2$  (green) on  $\mathcal{A}$  where we labels are available. (3) We learn a network  $G_{1 \rightarrow 2}$  that transform features from  $\mathcal{T}_1$  to  $\mathcal{T}_2$  on samples from  $\mathcal{A}$ . (4) We apply the transfer network on samples from  $\mathcal{B}$  to solve  $\mathcal{T}_2$  without the need for annotations.

## 4. Experimental Settings

We detail the experimental choices made when testing AT/DT, additional details will be reported in the supplementary material due to the lack of space.

**Tasks.** To validate the effectiveness of AT/DT, we select as  $\mathcal{T}_1$  and  $\mathcal{T}_2$  *semantic segmentation* and *monocular depth estimation*. We minimize a standard cross entropy loss to train a network on semantic segmentation while a standard  $L_1$  regression loss to train a network on monocular depth estimation. We choose these two tasks since they are closely related, as reported by recent works [29, 3, 4], and of clear interest for many practical applications like autonomous driving. Moreover, as both tasks require a structured output, they can be addressed by a similar network architecture with the only difference being the number of filters in the final layer: the number of classes for the semantic segmentation network and just one for the depth estimation.

**Datasets.** We consider four different datasets, two synthetic ones, and two real ones. We pick synthetic datasets as  $\mathcal{A}$  to learn the mapping across tasks thanks to the availability of free annotations. We use real dataset as  $\mathcal{B}$  to

benchmark the performance of AT/DT in challenging realistic conditions. As synthetic datasets we have used the six video sequences of the Synthia-SF dataset [17] (shortened Synthia) and rendered several other sequences with the Carla simulator [7]. For both datasets, we have split the data into a train, validation, and test set by subdividing them at the sequence level (*i.e.*, we have used different sequences as train, validation, and test). For the real datasets we have used images from the Kitti [11, 27, 10] and Cityscapes [5] benchmarks. Concerning Kitti, we have used the 200 images from the Kitti 2012 training set [11] to benchmark depth estimation algorithms and 200 images from the Kitti 2015 training set with semantic annotations recently released in [1]. Concerning Cityscapes, we have used the validation split to benchmark semantic segmentation algorithms and all the images in the training split. When training depth algorithms on Cityscapes we generate proxy labels by filtering SGM [18] disparities through confidence measures (left-right check) following a procedure similar to [34].

**Network Architecture.** Each task network is implemented as a dilated ResNet50 [42] that compress an image



to 1/16 of the input resolution to extract features. Then we use several bilinear up-sample and convolutional layers to regain resolution and get to the final prediction layer. All the layers of the network feature batch normalization. We implement the task transfer network ( $G_{1 \rightarrow 2}$ ) as a simple stack of convolutional and deconvolutional layers that reduce the inputs 1/4 of the spatial resolution before going back to the original scale.

**Evaluation Protocol.** For each test we select two domains (*i.e.*, two datasets, one referred as  $\mathcal{A}$  and the other as  $\mathcal{B}$ ) and one direction of task transfer, *i.e.*, from  $\mathcal{T}_1$  to  $\mathcal{T}_2$ . We will use  $Sem. \rightarrow Dep.$  when mapping features from semantic to depth and  $Dep. \rightarrow Sem.$  when switching the two tasks. For each configuration of dataset and tasks we use AT/DT to train a cross task network ( $G_{1 \rightarrow 2}$ ) following the protocol described in [Sec. 3.2](#), then measure its performance for  $\mathcal{T}_2$  on  $\mathcal{B}$ . We compare our method against a *Baseline* obtained training a network with supervision for  $\mathcal{T}_2$  in  $\mathcal{A}$  (*i.e.*,  $N_2^{\mathcal{A}}$ ) and testing it on  $\mathcal{B}$ .

**Metrics.** Our semantic segmentation networks predict eleven different classes corresponding to those available in the Carla simulator plus one additional class for ‘Sky’. To measure performance, we report two different global metrics: pixel accuracy, shortened *Acc.* (*i.e.*, the percentage of pixels with a correct label) and Mean Intersection Over Union, shortened *mIoU* (computed as detailed in [\[5\]](#)). To provide more insights on per-class gains we also report the *IoU* (intersection-over-union) score computed independently for each class.

When testing the depth estimation task we use the standard metrics described in [\[8\]](#): Absolute Relative Error (Abs Rel), Square Relative Error (Sq Rel), Root Mean Square Error (RMSE), logarithmic RMSE and three  $\delta$  accuracy scores ( $\delta_\alpha$  being the percentage of predictions whose maximum between ratio and inverse ratio with respect to the ground truth is lower than  $1.25^\alpha$ ).

## 5. Experimental Results

We subdivide the experimental results in three main sections: in [Sec. 5.1](#) and [Sec. 5.2](#) we transfer information between semantic segmentation and depth estimation in [Sec. 5.3](#), instead, we show preliminary result on the integration of AT/DT with domain adaptation techniques.

### 5.1. Depth to Semantics

Following the protocol detailed in [Sec. 4](#), we first test AT/DT when transferring knowledge from the *monocular depth estimation* task to the *semantic segmentation* task, and report the results in [Tab. 1](#). In this setup, we have complete supervision for both task in  $\mathcal{A}$  while only for depth estimation in  $\mathcal{B}$ . Therefore, for each configuration we report result obtained performing semantic segmentation on  $\mathcal{B}$  without any domain-specific supervision.

We begin our investigation studying the task transfer in a purely synthetic environment where we can have perfect annotations for all tasks and domains, *i.e.*, we use Synthia and Carla as  $\mathcal{A}$  and  $\mathcal{B}$ , respectively. The result obtained by AT/DT and a transfer learning baseline are reported in [Tab. 1-\(a\)](#). Comparing the two rows we can clearly see that our method boost performance by +9.02% and +6,64%, for mIoU and Acc, respectively, thanks to the additional knowledge transferred from the supervised depth task.

The same performance boost holds when considering a far more challenging domain transfer between synthetic and real data, *i.e.*, [Tab. 1-\(b\)](#) (Synthia  $\rightarrow$  Cityscapes) and [Tab. 1-\(c\)](#) (Carla  $\rightarrow$  Cityscapes). In both scenarios, our AT/DT improves the two averaged metrics (mIoU and Acc.) and most of the per class scores, with gain as large as +78,86% for the Road class in (b). Overall AT/DT consistently improves predictions for the more interesting classes in autonomous driving scenarios, *e.g.*, Road, Person... The main difficulties for AT/DT seems to be related to trying to transfer knowledge for classes where the depth estimation is particularly hard (*e.g.*, Vegetation where synthetic data have far from optimal annotations or thin structures like Poles and Fences). We wish to point out that in this scenario we do not use any annotation on the real Cityscapes data, since we automatically generate noisy proxy labels for depth from synchronized stereo frames following [\[34\]](#). Therefore all these results on real data are obtained leveraging only on image samples from the Cityscapes domain.

The top row of [Fig. 3](#) show qualitative results on Cityscapes where AT/DT produce clearly better disparity map than the baseline network.

### 5.2. Semantics to Depth

Following the protocol detailed in [Sec. 4](#) we test AT/DT when transferring features from *semantic segmentation* to *monocular depth estimation*. In this setup, we have complete supervision for both tasks in  $\mathcal{A}$  and only for semantic segmentation in  $\mathcal{B}$ . For each configuration we report in [Tab. 2](#) results obtained performing monocular depth estimation on  $\mathcal{B}$  without any domain-specific supervision.

The first pair of rows (*i.e.*, [Tab. 2-\(a\)](#)) reports results when transferring knowledge across two synthetic domains. The use of knowledge coming from semantic features helps AT/DT to predict better depth as clearly stated by the consistent improvement in all the seven metrics with respect to the baseline. The same gains do actually hold for tests concerning real datasets (*i.e.*, [Tab. 2-\(b\)](#) with Cityscapes and [Tab. 2-\(c\)](#) with Kitti) where the deployment of AT/DT always result in a clear advantage against the baseline.

We wish to point out how on [Tab. 2-\(c\)](#) we report a result where AT/DT use very few annotated samples from  $\mathcal{B}$  (*i.e.*, only the 200 images annotated with semantic labels released by [\[1\]](#)). Comparing [Tab. 2-\(c\)](#) to [Tab. 2-\(b\)](#) we can see

	$\mathcal{A}$	$\mathcal{B}$	Method	Road	Sidewalk	Walls	Fence	Person	Poles	Vegetation	Vehicles	Tr. Signs	Building	Sky	mIoU	Acc
(a)	Synthia	Carla	Baseline	63.94	54.87	15.21	<b>0.03</b>	13.55	12.78	<b>52.73</b>	27.34	4.88	50.24	79.73	34.12	73.36
	Synthia	Carla	AT/DT	<b>73.57</b>	<b>62.58</b>	<b>26.85</b>	0.00	<b>17.79</b>	<b>37.30</b>	35.27	<b>52.94</b>	<b>17.76</b>	<b>62.99</b>	<b>87.50</b>	<b>43.14</b>	<b>80.00</b>
(b)	Synthia	Cityscapes	Baseline	6.91	0.68	0.00	0.00	2.47	9.14	<b>3.19</b>	<b>8.90</b>	<b>0.81</b>	25.93	26.86	7.72	28.49
	Synthia	Cityscapes	AT/DT	<b>85.77</b>	<b>29.40</b>	<b>1.23</b>	0.00	<b>3.72</b>	<b>14.55</b>	1.87	8.85	0.38	<b>42.79</b>	<b>67.06</b>	<b>23.24</b>	<b>64.03</b>
(c)	Carla	Cityscapes	Baseline	71.87	<b>36.53</b>	3.99	<b>6.66</b>	24.33	22.20	66.06	<b>48.12</b>	7.60	60.22	69.05	37.88	74.61
	Carla	Cityscapes	AT/DT	<b>76.44</b>	32.24	<b>4.75</b>	5.58	<b>24.49</b>	<b>24.95</b>	<b>68.98</b>	40.49	<b>10.78</b>	<b>69.38</b>	<b>78.19</b>	<b>39.66</b>	<b>76.37</b>

Table 1: Experimental results of  $Dep. \rightarrow Sem.$  scenario. Best results highlighted in bold.

	$\mathcal{A}$	$\mathcal{B}$	Method	Lower is better				Higher is better		
				Abs Rel	Sq Rel	RMSE	RMSE log	$\delta_1$	$\delta_2$	$\delta_3$
(a)	Synthia	Carla	Baseline	0.632	8.922	13.464	0.664	0.323	0.578	0.733
	Synthia	Carla	AT/DT	<b>0.316</b>	<b>5.485</b>	<b>11.712</b>	<b>0.458</b>	<b>0.553</b>	<b>0.785</b>	<b>0.880</b>
(b)	Carla	Cityscapes	Baseline	0.667	13.500	16.875	0.593	0.276	0.566	0.770
	Carla	Cityscapes	AT/DT	<b>0.394</b>	<b>5.837</b>	<b>13.915</b>	<b>0.435</b>	<b>0.337</b>	<b>0.749</b>	<b>0.899</b>
(c)	Carla	Kitti	Baseline	0.500	10.602	10.772	0.487	0.384	0.723	0.853
	Carla	Kitti	AT/DT	<b>0.439</b>	<b>8.263</b>	<b>9.148</b>	<b>0.421</b>	<b>0.483</b>	<b>0.788</b>	<b>0.891</b>

Table 2: Experimental results of  $Sem. \rightarrow Dep.$  scenario. Best results highlighted in bold.

how the low data regime of Kitti results in slightly smaller gains in performance; nevertheless AT/DT consistently improves compared to the baseline across all the seven metrics. We believe that these results provide some assurances on the effectiveness of AT/DT with respect to the amount of available data per task. Finally, the bottom row of Fig. 3 shows qualitative results on monocular depth estimation on Cityscapes, we can clearly see the big advantage of AT/DT over the baseline, especially on far objects.

### 5.3. Integration with Domain Adaptation

All the results of Sec. 5.1 and Sec. 5.2 are obtained learning a mapping function across tasks on a domain and deploying it on another one. Therefore, the transfer network  $G_{1 \rightarrow 2}$  we learn, as well as the baseline we are considering, can indeed suffer from domain shift issues. Fortunately, the domain adaptation literature provides several different strategies to overcome domain shifts that are complementary to our AT/DT. Here we wish to provide some preliminary results on how the two approaches can be combined together. Following recent trends in literature, we consider a pixel-level domain adaptation technique, *i.e.*, CycleGAN [47], that transform images from  $\mathcal{B}$  to make them more similar to samples from  $\mathcal{A}$ .

In Tab. 3, we report results obtained for a  $Dep. \rightarrow Sem.$

scenario using Carla as  $\mathcal{A}$  and Cityscapes as  $\mathcal{B}$ . The pixel level domain alignment of CycleGAN (row (c)) proves particularly effective in this scenario, providing a huge boost when compared to the baseline (row (a)); even greater than the gain granted by AT/DT (row (b)). However, we can see how the best averaged results (*i.e.*, mIoU and Acc.) can be obtained combining our cross task framework (AT/DT) with the pixel level domain adaptation provided by CycleGAN (row (d)). Considering the scores on single classes, instead, there is no clear winner among the four considered methods, with different algorithms providing better accuracy for different classes.

In Tab. 4 we report results obtained on a  $Sem. \rightarrow Dep.$  scenario using the same pair of domains and the same four methods. Surprisingly, when targeting depth estimation CycleGAN (row (c)) is not as effective as before and actually worsen significantly the performance of the baseline (row (a)). Our AT/DT is instead more robust to the task being addressed and in this scenario is able to improve the baseline when combined with CycleGAN (row (d)) and obtain the best overall results when applied alone (row (a)).

## 6. Additional Experiments

We report here additional tests to shine a light on some of the design choices made when developing AT/DT

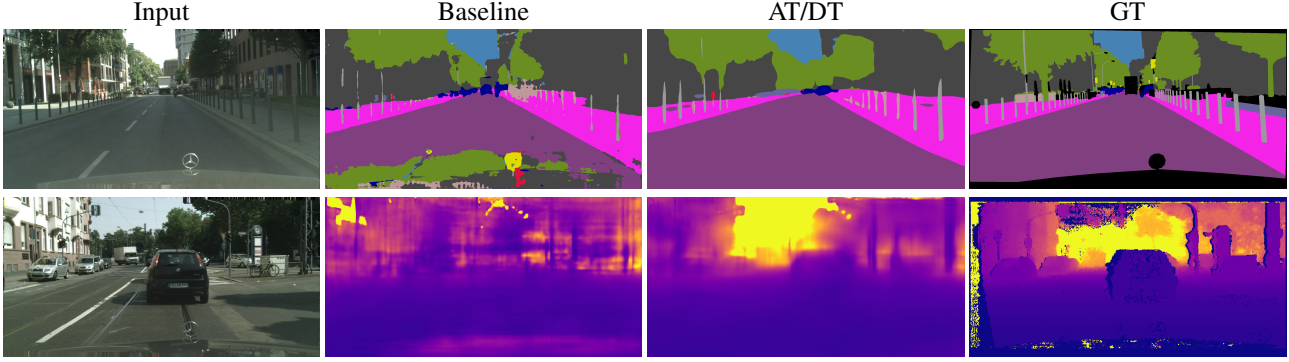


Figure 3: Qualitative results for  $\mathcal{A}$ : Carla to  $\mathcal{B}$ : Cityscapes. First row shows  $Dep. \rightarrow Sem.$  scenario while second row shows  $Sem. \rightarrow Dep.$  setting. From left to right RGB input, baseline prediction, AT/DT prediction, ground-truth images.

Method	Road	Sidewalk	Walls	Fence	Person	Poles	Vegetation	Vehicles	Tr. Signs	Building	Sky	mIoU	Acc
(a) Baseline	71.87	36.53	3.99	<b>6.66</b>	24.33	22.20	66.06	48.12	7.60	60.22	69.05	37.88	74.61
(b) AT/DT	76.44	32.24	4.75	5.58	24.49	<b>24.95</b>	68.98	40.49	<b>10.78</b>	69.38	<b>78.19</b>	39.66	76.37
(c) CycleGAN	81.58	39.15	<b>6.08</b>	5.31	<b>30.22</b>	21.73	<b>77.71</b>	50.00	8.33	68.35	77.22	42.33	80.93
(d) AT/DT + CycleGAN	<b>85.19</b>	<b>41.37</b>	5.44	3.02	29.90	24.07	71.93	<b>58.09</b>	7.53	<b>70.90</b>	77.78	<b>43.20</b>	<b>81.92</b>

Table 3: Experimental results of integration with domain adaptation techniques. We show results of  $\mathcal{A}$ : Carla to  $\mathcal{B}$  Cityscapes: and  $Dep. \rightarrow Sem.$  scenario. Best results highlighted in bold.

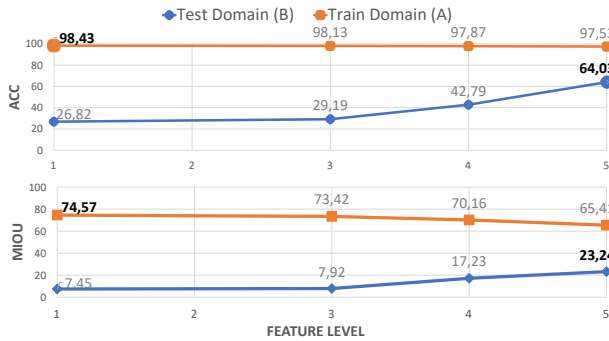


Figure 4: Study on the optimal feature level for task transfer between  $\mathcal{A}$ : Synthia to  $\mathcal{B}$ : Cityscapes and  $Dep. \rightarrow Sem.$  scenario. Deeper levels correspond to higher generalization performances.

### 6.1. Study on the transfer level

For all the previous tests we split  $N$  between  $E$  and  $D$  at the network layer at lowest spatial resolution. We pick this split based on the intuition that deeper convolutional layers yield more abstract representations, thus less correlated to specific domain information, while lower level features are more domain dependent. Therefore, learning  $G_{1 \rightarrow 2}$  at

lower levels should lead to less generalization ability across domains.

To experimentally validate this intuition, we conduct additional experiments aimed at measuring performance for the  $Dep. \rightarrow Sem.$  scenario (Synthia  $\rightarrow$  Cityscapes) when varying the network layer at which we split  $N$  into  $E$  and  $D$ . We consider four different feature levels corresponding to residual blocks at increasing depth in ResNet50. For each one of them we train a transfer network on samples from domain  $\mathcal{A}$  and then measure  $mIoU$  and  $Acc.$  on unseen images from  $\mathcal{A}$  and  $\mathcal{B}$ . The results are plotted in Fig. 4.

Considering  $Acc.$  (top plot) we can see how in-domain performance are almost equivalent at the different feature level (orange line), while cross-domain performance increase when considering deeper feature levels (blue line). This pattern is even more pronounced when considering  $mIoU$  (bottom plot) where in-domain performance actually decreases alongside with deeper feature, whilst cross-domain performance increase. We believe that these results validate our intuition that deeper features are less domain specific and may lead to better generalization to unseen domains.

	Method	Lower is better				Higher is better		
		Abs Rel	Sq Rel	RMSE	RMSE log	$\delta_1$	$\delta_2$	$\delta_3$
(a)	Baseline	0.667	13.499	16.875	0.593	0.276	0.566	0.770
(b)	AT/DT	<b>0.394</b>	<b>5.837</b>	<b>13.915</b>	<b>0.435</b>	<b>0.337</b>	<b>0.749</b>	<b>0.899</b>
(c)	CycleGAN	0.943	27.026	21.666	0.695	0.218	0.478	0.690
(d)	AT/DT+CycleGAN	0.563	10.789	15.636	0.489	0.247	0.668	0.861

Table 4: Experimental results of comparison and integration with domain adaptation techniques. We show results of  $\mathcal{A}$ : Carla to  $\mathcal{B}$ : Cityscapes and  $Sem. \rightarrow Dep.$  scenario. Best results highlighted in bold.

Shared	Domain	mIoU	Acc.
$\times$	$\mathcal{A}$	61.73	97.02
$\checkmark$	$\mathcal{A}$	65.41	97.53
$\times$	$\mathcal{B}$	6.42	29.36
$\checkmark$	$\mathcal{B}$	23.24 ( <b>+16.82</b> )	64.03 ( <b>+34.67</b> )

Table 5: Study on Shared vs Non-Shared  $N_1^{A \cup B}$ . We show a  $\mathcal{A}$ : Synthia to  $\mathcal{B}$ : Carla and  $Dep. \rightarrow Sem.$  scenario. Performance improvement highlighted in bold.

## 6.2. Shared vs Non-Shared $N_1$

Throughout this work we have always trained a single network for  $\mathcal{T}_1$  with samples from  $\mathcal{A}$  and  $\mathcal{B}$ . The rationale behind this choice is to have a single feature extractor for both domains such that  $G_{1 \rightarrow 2}$  trained only on samples from  $\mathcal{A}$  would be able to generalize well to samples from  $\mathcal{B}$  as they are sampled from a similar distribution.

Here we experimentally validate this intuition by comparing a shared  $N_1^{A \cup B}$  against the use of two separate networks, one trained on samples from  $\mathcal{A}$  ( $N_1^A$ ) and the other with samples from  $\mathcal{B}$  ( $N_1^B$ ). We consider a  $Dep. \rightarrow Sem.$  scenario where we use Synthia as domain  $\mathcal{A}$  and Cityscapes as  $\mathcal{B}$ . In Tab. 5 we report the *mIoU* and *Acc.* achieved on unseen samples from the two domains. On the training domain  $\mathcal{A}$  both methods are able to obtain good results, with a slight advantage for the shared network, probably thanks to the higher variety of data used for training. However when moving on the completely different domain  $\mathcal{B}$  it is clear that maintaining the same feature extractor is of crucial importance to be able to use the same  $G_{1 \rightarrow 2}$ . This test suggests the interesting findings that feature extracted by the exact same network architecture trained for the exact same tasks in two different domains are quite different. Therefore to correctly apply  $G_{1 \rightarrow 2}$  we need to take into account these difficulties.

## 6.3. Batch Normalization

We explore the impact on the performance of using task networks with or without batch normalization layers [21].

Batchnorm	Domain	mIoU	Acc.
$\times$	$\mathcal{A}$	72.48	98.09
$\checkmark$	$\mathcal{A}$	65.41	97.53
$\times$	$\mathcal{B}$	22.75	58.29
$\checkmark$	$\mathcal{B}$	23.24 ( <b>+0.49</b> )	64.03 ( <b>+5.74</b> )

Table 6: Ablation Study on Batch Normalization. We show a  $\mathcal{A}$ : Synthia to  $\mathcal{B}$ : Cityscapes and  $Dep. \rightarrow Sem.$  scenario. Performance improvement highlighted in bold.

Our intuition is that the introduction of batch normalization should render the feature representation more similar across domains and therefore help the task transfer network  $G_{1 \rightarrow 2}$ . In Tab. 6 we report results in  $Dep. \rightarrow Sem.$  scenario when employing Synthia as  $\mathcal{A}$  and Cityscapes as  $\mathcal{B}$ . As expected, batch normalization yields representations more similar between domains, thus leading to better generalization performances (*i.e.*, on  $\mathcal{B}$ ). Counter-intuitively, we can also notice that results in  $\mathcal{A}$  are worse with batch normalization, possibly showing that transforming features from  $\mathcal{T}_1$  to  $\mathcal{T}_2$  is harder when those features lie on a more constrained space.

## 7. Conclusion and Future Works

We have shown that it is possible to learn a mapping function to transform deep representations suitable for specific tasks into others amenable to different ones. This mapping function is learned on a specific training set and not only generalizes to unseen data from the same domain but also to new samples from a different domain. This strategy allows for leveraging on easy to annotate domains (*e.g.*, synthetic data) in order to solve tasks in scenarios where annotations would be costly. We have shown promising results obtained by applying our framework to two tasks (semantic segmentation and monocular depth estimation) and four quite different domains (two synthetic domains and two real domains). In future works, we wish to investigate the effectiveness and robustness of our framework when addressing other tasks. In this respect, *Taskonomy* [43] may guide us in identifying tightly related visual tasks likely to enable effec-



tive transfer of learned representations. We have also shown preliminary results concerning how our framework may be fused with standard domain adaptation strategies in order to further ameliorate performance. We believe that the search for the best strategy to fuse the two worlds is a novel and exciting research avenue set forth by our paper.

## References

- [1] H. Alhajja, S. Mustikovela, L. Mescheder, A. Geiger, and C. Rother. Augmented reality meets computer vision: Efficient data generation for urban driving scenes. *International Journal of Computer Vision (IJCV)*, 2018. 4, 5
- [2] K. Bousmalis, N. Silberman, D. Dohan, D. Erhan, and D. Krishnan. Unsupervised pixel-level domain adaptation with generative adversarial networks. *2017 IEEE Conference on Computer Vision and Pattern Recognition (CVPR)*, Jul 2017. 2
- [3] S. Chennupati, G. Sistu, S. Yogamani, and S. Rawashdeh. Auxnet: Auxiliary tasks enhanced semantic segmentation for automated driving, 2019. 2, 4
- [4] R. Cipolla, Y. Gal, and A. Kendall. Multi-task learning using uncertainty to weigh losses for scene geometry and semantics. *2018 IEEE/CVF Conference on Computer Vision and Pattern Recognition*, Jun 2018. 2, 4
- [5] M. Cordts, M. Omran, S. Ramos, T. Rehfeld, M. Enzweiler, R. Benenson, U. Franke, S. Roth, and B. Schiele. The cityscapes dataset for semantic urban scene understanding. In *The IEEE Conference on Computer Vision and Pattern Recognition (CVPR)*, June 2016. 2, 4, 5
- [6] C. Doersch and A. Zisserman. Multi-task self-supervised visual learning. *2017 IEEE International Conference on Computer Vision (ICCV)*, Oct 2017. 2
- [7] A. Dosovitskiy, G. Ros, F. Codevilla, A. Lopez, and V. Koltun. CARLA: An open urban driving simulator. In *Proceedings of the 1st Annual Conference on Robot Learning*, pages 1–16, 2017. 2, 4
- [8] D. Eigen, C. Puhrsch, and R. Fergus. Depth map prediction from a single image using a multi-scale deep network. In *Advances in neural information processing systems*, pages 2366–2374, 2014. 5
- [9] Y. Ganin and V. Lempitsky. Unsupervised domain adaptation by backpropagation. In *International Conference on Machine Learning*, pages 1180–1189, 2015. 2
- [10] A. Geiger, P. Lenz, C. Stiller, and R. Urtasun. Vision meets robotics: The kitti dataset. *International Journal of Robotics Research (IJRR)*, 2013. 4
- [11] A. Geiger, P. Lenz, and R. Urtasun. Are we ready for autonomous driving? the kitti vision benchmark suite. In *Computer Vision and Pattern Recognition (CVPR), 2012 IEEE Conference on*, pages 3354–3361. IEEE, 2012. 2, 4
- [12] B. Gong, Y. Shi, F. Sha, and K. Grauman. Geodesic flow kernel for unsupervised domain adaptation. In *Computer Vision and Pattern Recognition (CVPR), 2012 IEEE Conference on*, pages 2066–2073. IEEE, 2012. 2
- [13] R. Gopalan, R. Li, and R. Chellappa. Domain adaptation for object recognition: An unsupervised approach. In *Computer Vision (ICCV), 2011 IEEE International Conference on*, pages 999–1006. IEEE, 2011. 2
- [14] M. Guo, A. Haque, D.-A. Huang, S. Yeung, and L. Fei-Fei. Dynamic task prioritization for multitask learning. In *The European Conference on Computer Vision (ECCV)*, September 2018. 2
- [15] K. He, R. Girshick, and P. Dollr. Rethinking imagenet pre-training, 2018. 2
- [16] K. He, G. Gkioxari, P. Dollar, and R. Girshick. Mask r-cnn. *2017 IEEE International Conference on Computer Vision (ICCV)*, Oct 2017. 2
- [17] D. Hernandez-Juarez, L. Schneider, A. Espinosa, D. Vazquez, A. M. Lopez, U. Franke, M. Pollefeys, and J. C. Moure. Slanted stixels: Representing san francisco steepest streets. In *British Machine Vision Conference (BMVC), 2017*, 2017. 2, 4
- [18] H. Hirschmuller. Accurate and efficient stereo processing by semi-global matching and mutual information. In *Computer Vision and Pattern Recognition, 2005. CVPR 2005. IEEE Computer Society Conference on*, volume 2, pages 807–814. IEEE, 2005. 4
- [19] J. Hoffman, E. Tzeng, T. Park, J.-Y. Zhu, P. Isola, K. Saenko, A. A. Efros, and T. Darrell. Cycada: Cycle-consistent adversarial domain adaptation, 2017. 2
- [20] J. Hoffman, D. Wang, F. Yu, and T. Darrell. Fcns in the wild: Pixel-level adversarial and constraint-based adaptation. *arXiv preprint arXiv:1612.02649*, 2016. 2
- [21] S. Ioffe and C. Szegedy. Batch normalization: Accelerating deep network training by reducing internal covariate shift. In *Proceedings of the 32Nd International Conference on International Conference on Machine Learning - Volume 37, ICML'15*, pages 448–456. JMLR.org, 2015. 8
- [22] P. Isola, J.-Y. Zhu, T. Zhou, and A. A. Efros. Image-to-image translation with conditional adversarial networks. In *The IEEE Conference on Computer Vision and Pattern Recognition (CVPR)*, July 2017. 2
- [23] M. Klodt and A. Vedaldi. Supervising the new with the old: learning sfm from sfm. In *Proceedings of the European Conference on Computer Vision (ECCV)*, pages 698–713, 2018. 2
- [24] I. Kokkinos. Ubernet: Training a universal convolutional neural network for low-, mid-, and high-level vision using diverse datasets and limited memory. *2017 IEEE Conference on Computer Vision and Pattern Recognition (CVPR)*, Jul 2017. 2
- [25] M. Long, Y. Cao, J. Wang, and M. Jordan. Learning transferable features with deep adaptation networks. In *Proceedings of the 32nd International Conference on Machine Learning*, volume 37 of *Proceedings of Machine Learning Research*, pages 97–105. PMLR, 2015. 2
- [26] Z. Luo, Y. Zou, J. Hoffman, and L. F. Fei-Fei. Label efficient learning of transferable representations across domains and tasks. In *Advances in Neural Information Processing Systems*, pages 165–177, 2017. 2
- [27] M. Menze and A. Geiger. Object scene flow for autonomous vehicles. In *Conference on Computer Vision and Pattern Recognition (CVPR)*, 2015. 2, 4

- [28] A. Pal and V. N. Balasubramanian. Zero-shot task transfer, 2019. [2](#)
- [29] P. Z. Ramirez, M. Poggi, F. Tosi, S. Mattoccia, and L. Di Stefano. Geometry meets semantics for semi-supervised monocular depth estimation. *arXiv preprint arXiv:1810.04093*, 2018. [2](#), [4](#)
- [30] P. Z. Ramirez, A. Tonioni, and L. D. Stefano. Exploiting semantics in adversarial training for image-level domain adaptation, 2018. [2](#)
- [31] S. Ren, K. He, R. Girshick, and J. Sun. Faster r-cnn: Towards real-time object detection with region proposal networks. *IEEE Transactions on Pattern Analysis and Machine Intelligence*, 39(6):11371149, Jun 2017. [2](#)
- [32] S. Sankaranarayanan, Y. Balaji, A. Jain, S. N. Lim, and R. Chellappa. Learning from synthetic data: Addressing domain shift for semantic segmentation. *2018 IEEE/CVF Conference on Computer Vision and Pattern Recognition*, Jun 2018. [2](#)
- [33] A. Shrivastava, T. Pfister, O. Tuzel, J. Susskind, W. Wang, and R. Webb. Learning from simulated and unsupervised images through adversarial training. In *The IEEE Conference on Computer Vision and Pattern Recognition (CVPR)*, 2017. [2](#)
- [34] A. Tonioni, M. Poggi, S. Mattoccia, and L. Di Stefano. Unsupervised adaptation for deep stereo. In *Proceedings of the IEEE International Conference on Computer Vision*, pages 1605–1613, 2017. [2](#), [4](#), [5](#)
- [35] Y.-H. Tsai, W.-C. Hung, S. Schuler, K. Sohn, M.-H. Yang, and M. Chandraker. Learning to adapt structured output space for semantic segmentation. *2018 IEEE/CVF Conference on Computer Vision and Pattern Recognition*, Jun 2018. [2](#)
- [36] E. Tzeng, J. Hoffman, T. Darrell, and K. Saenko. Simultaneous deep transfer across domains and tasks. In *Proceedings of the IEEE International Conference on Computer Vision*, pages 4068–4076, 2015. [2](#)
- [37] E. Tzeng, J. Hoffman, K. Saenko, and T. Darrell. Adversarial discriminative domain adaptation. In *Computer Vision and Pattern Recognition (CVPR)*, 2017. [2](#)
- [38] M. Wang and W. Deng. Deep visual domain adaptation: A survey. *Neurocomputing*, 312:135–153, 2018. [1](#)
- [39] M. Wang and W. Deng. Deep visual domain adaptation: A survey. *Neurocomputing*, 312:135153, Oct 2018. [2](#)
- [40] N. Yang, R. Wang, J. Stuckler, and D. Cremers. Deep virtual stereo odometry: Leveraging deep depth prediction for monocular direct sparse odometry. In *Proceedings of the European Conference on Computer Vision (ECCV)*, pages 817–833, 2018. [2](#)
- [41] J. Yosinski, J. Clune, Y. Bengio, and H. Lipson. How transferable are features in deep neural networks? In *Advances in neural information processing systems*, pages 3320–3328, 2014. [2](#)
- [42] F. Yu, V. Koltun, and T. Funkhouser. Dilated residual networks. In *Computer Vision and Pattern Recognition (CVPR)*, 2017. [4](#)
- [43] A. R. Zamir, A. Sax, W. Shen, L. J. Guibas, J. Malik, and S. Savarese. Taskonomy: Disentangling task transfer learning. In *Proceedings of the IEEE Conference on Computer Vision and Pattern Recognition*, pages 3712–3722, 2018. [1](#), [2](#), [3](#), [8](#)
- [44] Y. Zhang, P. David, and B. Gong. Curriculum domain adaptation for semantic segmentation of urban scenes. In *The IEEE International Conference on Computer Vision (ICCV)*, 2017. [2](#)
- [45] Y. Zhang, Z. Qiu, T. Yao, D. Liu, and T. Mei. Fully convolutional adaptation networks for semantic segmentation. *2018 IEEE/CVF Conference on Computer Vision and Pattern Recognition*, Jun 2018. [2](#)
- [46] C. Zheng, T.-J. Cham, and J. Cai. T2net: Synthetic-to-realistic translation for solving single-image depth estimation tasks. In *The European Conference on Computer Vision (ECCV)*, September 2018. [2](#)
- [47] J.-Y. Zhu, T. Park, P. Isola, and A. A. Efros. Unpaired image-to-image translation using cycle-consistent adversarial networks. In *The IEEE International Conference on Computer Vision (ICCV)*, Oct 2017. [2](#), [6](#)

# Supplementary material for Learning Across Tasks and Domains

Pierluigi Zama Ramirez, Alessio Tonioni, Samuele Salti, Luigi di Stefano  
Department of Computer Science and Engineering (DISI)  
University of Bologna, Italy

{pierluigi.zama, alessio.tonioni, samuele.salti, luigi.distefano}@unibo.it

## 1. Additional Experimental Results

We report here additional experiments to assess the contribution of the different components of AT/DT. In [Sec. 1.1](#) we conduct a study on the performance achievable on the training domain  $\mathcal{A}$  with  $G_{1 \rightarrow 2}$ . In [Sec. 1.2](#) we provide additional details and results on the integration of AT/DT with domain adaptation techniques. In [Sec. 1.3](#) we report qualitative results using as target task ( $\mathcal{T}_2$ ) the normal estimation, where we do not have ground truth labels to evaluate results on real data. Finally, in [Sec. 2](#) and [Sec. 3](#) we provide additional details about the training and evaluation processes.

### 1.1. Train domain performance of $G_{1 \rightarrow 2}$

Our framework has to overcome two different nuisances to provide an effective solution for the task lacking supervision in the target domain: the translation of features between tasks and the change of domain. In this section, we are interested in isolating the loss in performance due to the first issue, which will also provide some hints on the importance of the second one. In other words, we are trying to answer the question: *How well are we effectively learning to translate deep representations?*

To focus only on our effectiveness in transferring representations, we consider a test set of images from  $\mathcal{A}$  and compare AT/DT and  $N_2^A$  (the network trained on domain  $\mathcal{A}$  for  $\mathcal{T}_2$ ). As the test data are sampled from the same domain as the training data, we do not have errors due to the domain change and we can use the gap in performance between the two algorithms as a measure of the effectiveness of our framework in transferring representations. As we wish to evaluate both semantic segmentation and depth estimation, we select the Synthia domain as  $\mathcal{A}$ , for which we have all labels available, and Cityscapes as  $\mathcal{B}$ . In [Tab. 1](#) we report the results when transferring deep representations in the  $Dep. \rightarrow Sem.$  scenario, while in [Tab. 2](#) in the  $Sem. \rightarrow Dep.$  scenario.

On [Tab. 1](#) we can see how transferring deep representations from  $\mathcal{T}_1$  to  $\mathcal{T}_2$  with AT/DT results in a small loss in performance when compared to  $N_2^A$ . In particular, the largest performance drops are related to classes dealing with small

objects, like ‘Fence’, ‘Poles’ and ‘Traffic Sign’, that might get lost transferring features at the smallest spatial resolution in the network. These results suggest that a multi-scale transfer strategy would be a direction worth exploring in future works to better recover small details when transferring representations. Nevertheless, comparing the final pixel accuracy (Acc.), AT/DT lose only 1% using a feature extractor trained for a completely different task.

In [Tab. 2](#) AT/DT obtains again performance close to  $N_2^A$ . For some metrics, it even delivers better performance than  $N_2^A$ . This somewhat surprising result can be explained by the difference in training sets between the two algorithms: AT/DT uses as feature extractor  $N_1^{A \cup B}$  that has been trained with samples from both  $\mathcal{A}$  and  $\mathcal{B}$ , *i.e.* with a larger and more varied training set than that used by  $N_2^A$ . Therefore, the encoder of  $N_1^{A \cup B}$  might learn a more general feature extractor than that of  $N_2^A$ , this resulting in better performance when applied on unseen data. AT/DT can successfully leverage on this better feature extractor and obtain slightly better performance when transferring them to  $\mathcal{T}_2$ .

The same reasoning may be applied to the results of [Tab. 1](#). However, in this case, the shared encoder of  $N_1^{A \cup B}$  has been partially trained with noisy ground truth depth labels on samples from  $\mathcal{B}$ . The introduction of partial noise in the training process might harm the learning of  $N_1^{A \cup B}$  and explain the small gap in performance. Moreover, as stated above, due to the transferring of features at low resolution, AT/DT might struggle to transfer small structure in the image (*e.g.*, ‘poles’, ‘traffic sign’...). However, wrong predictions on this kind of small structures do not harm much the depth estimation metrics (*i.e.*, few pixels considered), though they have a larger impact on the mIoU metric considered for semantic segmentation. Finally, as stated in [\[2\]](#), the advantages yielded by semantic information to depth estimation are larger than the gains attainable going in the other direction, this motivating the slight difference in performance across the two scenarios.

Overall, results reported in [Tab. 2](#) and [Tab. 1](#) show that our framework is indeed learning to transfer deep representations effectively and that it is possible to approximate

$\mathcal{A}$	Method	Road	Sidewalk	Walls	Fence	Person	Poles	Vegetation	Vehicles	Tr. Signs	Building	Sky	mIoU	Acc
Synthia	$N_2^A$	<b>99.23</b>	<b>87.16</b>	<b>92.67</b>	<b>28.62</b>	<b>48.53</b>	<b>63.54</b>	<b>85.02</b>	<b>88.92</b>	<b>52.67</b>	<b>96.91</b>	<b>98.39</b>	<b>76.52</b>	<b>98.45</b>
Synthia	AT/DT	98.34	76.09	84.99	1.06	29.25	45.57	80.15	85.72	25.31	95.53	97.45	65.41	97.53

Table 1: Experimental results of  $Dep. \rightarrow Sem.$  scenario using as domain  $\mathcal{A}$  the Synthia dataset. Best results highlighted in bold.

$\mathcal{A}$	Method	Lower is better				Higher is better		
		Abs Rel	Sq Rel	RMSE	RMSE log	$\delta_1$	$\delta_2$	$\delta_3$
Synthia	$N_2^A$	0.138	<b>1.212</b>	<b>4.759</b>	0.825	<b>0.864</b>	0.952	0.970
Synthia	AT/DT	<b>0.135</b>	1.271	5.061	<b>0.634</b>	0.863	<b>0.958</b>	<b>0.977</b>

Table 2: Experimental results of  $Sem. \rightarrow Dep.$  scenario using as domain  $\mathcal{A}$  the Synthia dataset. Best results highlighted in bold.

$G_{1 \rightarrow 2}$  with a neural network like the one we proposed. This is further validated in Fig. 1, where we report two t-SNE[3] plots of deep features extracted by  $N_1^{A \cup B}$  (in pink),  $N_2^A$  (in blue) alongside with the features transformed by  $G_{1 \rightarrow 2}$  (in red). All features are computed on image samples from the test set described above, *i.e.* samples unseen at training time. Therefore,  $G_{1 \rightarrow 2}$  takes as input pink points and produces red points that should be as close as possible to the blue points. Indeed, the two plots show how our task transfer network can successfully produce features suitable for  $\mathcal{T}_2$ .

## 1.2. Integration with Domain Adaptation

We report here additional details on how we have used CycleGAN [5] to address domain adaptation.

We train CycleGAN to transform images from Carla ( $\mathcal{A}$ ) to Cityscapes ( $\mathcal{B}$ ) and vice versa. The network is trained using the original author implementation<sup>1</sup> for 200k steps on random image crops of  $400 \times 400$  resolution. We use the same hyper-parameters settings proposed in the original paper.

Once trained, we transform the Cityscapes dataset to the Carla style generating a new *CityscapesLikeCarla* dataset which we will call *BlikeA* domain (see Fig. 2). The baseline is then obtained testing  $N_2^A$  with the validation set of *BlikeA*. To integrate AT/DT with CycleGAN, we train a  $N_1^{A \cup \{BlikeA\}}$  on both  $\mathcal{A}$  and *BlikeA* at step 1 of AT/DT. Then, at step 4, to infer the predictions for  $\mathcal{T}_2$  on  $\mathcal{B}$ , we employ the validation set of *BlikeA* as done for the baseline. To summarize we train the shared source network on samples obtained from  $\mathcal{A}$  and *BlikeA*, then we test all net-

<sup>1</sup><https://github.com/junyanz/pytorch-CycleGAN-and-pix2pix>

works on the test set of *BlikeA* (*i.e.*, Cityscapes images transformed to look like those from Carla).

In Fig. 3 we show some qualitative results obtained when combining AT/DT together with the pixel level domain adaptation obtained through CycleGAN. Comparing the results in the  $Sem. \rightarrow Dep.$  scenario (first row) with those obtained in a  $Dep. \rightarrow Sem.$  scenario (second row) we can see how CycleGAN is very effective when targeting the semantic segmentation tasks, less effective when targeting a depth estimation task. AT/DT, instead, consistently produce better predictions than the baseline across the two considered tasks.

## 1.3. Additional tasks

In Fig. 4 we report additional qualitative results when using as  $\mathcal{T}_1$  semantic estimation and as  $\mathcal{T}_2$  normal estimation with Carla as  $\mathcal{A}$  and Cityscapes as  $\mathcal{B}$ . The results confirm the findings of the semantic to depth scenario with AT/DT producing clearly better prediction than the baseline network. We report only qualitative results due to the lack of annotations to validate normal estimation on the real Cityscapes data.

## 2. Details on the training process

Upon acceptance, we will release our code to encourage further research in this exciting new field.

Our task networks consist of a ResNet50 as the encoder and a stack of 3 series of bilinear upsampler followed by one convolution as the decoder. Our ResNet50 use dilated convolution with rate 2 and 4 in the last two residual blocks similar to what proposed in DRN [4]. We trained our  $N_1^{A \cup B}$  and  $N_2^A$  until the loss stabilize with batch size 8 and crop  $512 \times 512$ .



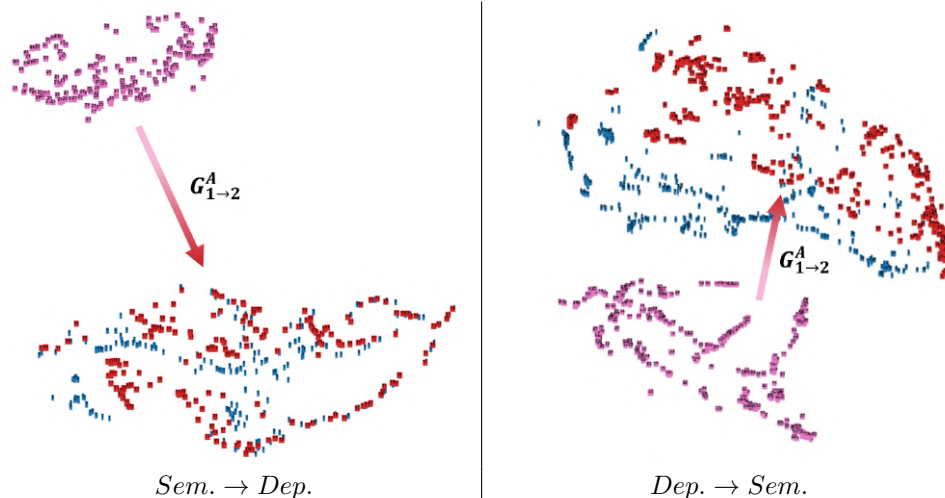


Figure 1: t-SNE [3] plots of deep features computed on  $\mathcal{A}$ . Pink denotes the features extracted for  $\mathcal{T}_1$ , i.e.  $E_1^{A \cup B}(x_a)$ . Blue features extracted for  $\mathcal{T}_2$ , i.e.  $E_2^A(x_a)$ . Red the prediction obtained by the feature transfer network  $G_{1 \rightarrow 2}(E_1^{A \cup B}(x_a))$ . Therefore, the red points are the transformations of the pink points according to  $G_{1 \rightarrow 2}$ . With an ideal  $G_{1 \rightarrow 2}$  red and blue points would perfectly overlap, here we can see that unfortunately this is not the case. Nevertheless our transfer function successfully transform pink features to make them closer to blue ones.

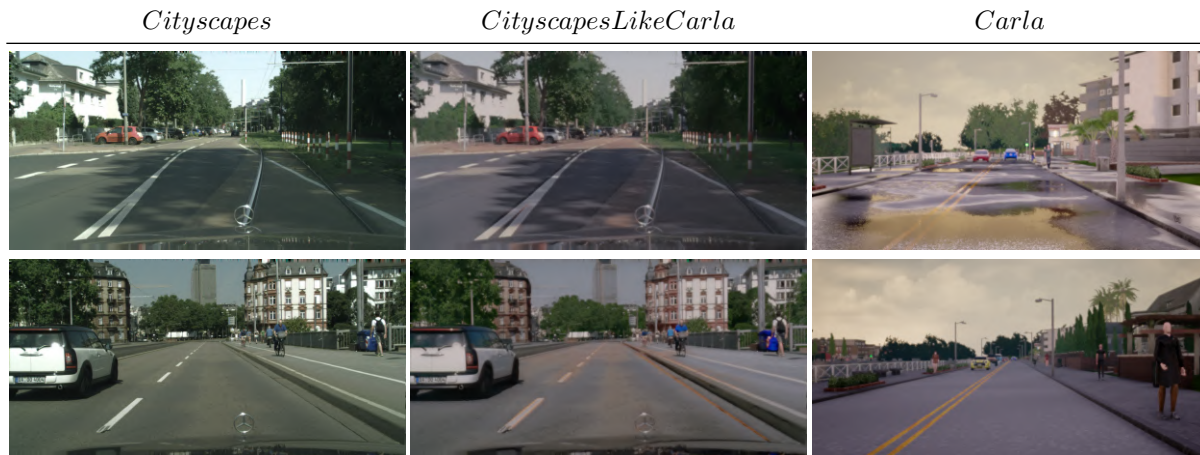


Figure 2: Images obtained applying CycleGAN to make Cityscapes samples similar to those of Carla. From left to right: samples from Cityscapes, corresponding image from *CityscapesLikeCarla* obtained by CycleGAN, similar samples from Carla

We use Adam [1] as optimizer with a linear decaying learning rate  $10^{-4}$  and  $\beta_1 = 0.9$ .

Our  $G_{1 \rightarrow 2}$  is composed by a stack of 6 convolutional layers with kernel side 3 going down to a quarter of the input resolution and then upsampling back to original resolution. We train this network for 100k iterations with batch size 1 and random crops of  $512 \times 512$  resolution. We use Adam [1] as optimizer with learning rate  $10^{-5}$ .

### 3. Details on the evaluation process

We perform all the evaluation at the original image resolution for Cityscapes, Carla and Synthia. Instead, for Kitti, we consider a central crop with size  $320 \times 1216$  due to the varying size of images. We divide the evaluation protocol by task.

**Semantic Segmentation** We train and evaluate the semantic segmentation task on 11 classes, the 10 defined by the Carla framework<sup>2</sup> plus the additional ‘Sky’ class that

<sup>2</sup><https://github.com/carla-simulator/carla/>



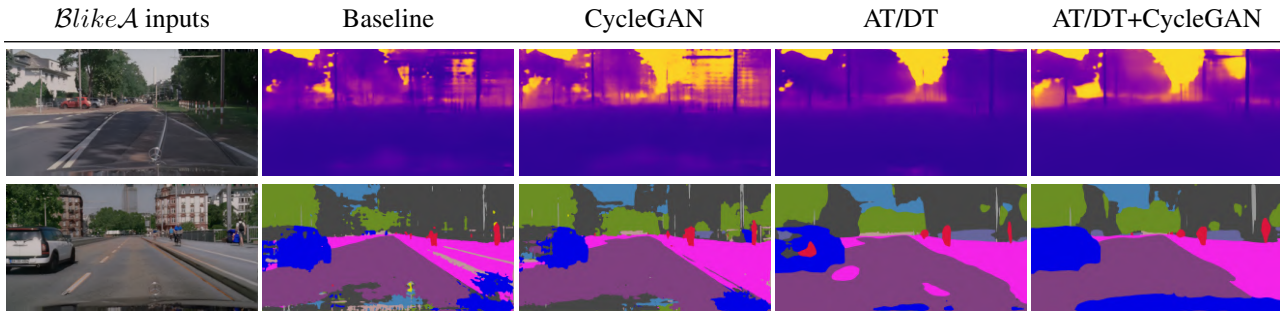


Figure 3: Qualitative results on the Cityscapes dataset in a *Sem.*  $\rightarrow$  *Dep.* scenario (first row) and *Dep.*  $\rightarrow$  *Sem.* scenario (second row). From left to right: *BlikeA* inputs, predictions obtained by a transfer learning baseline, by a domain adaptation baseline (CycleGAN[5]), by our framework (AT/DT) and by our framework aided by domain adaptation (AT/DT+CycleGAN).

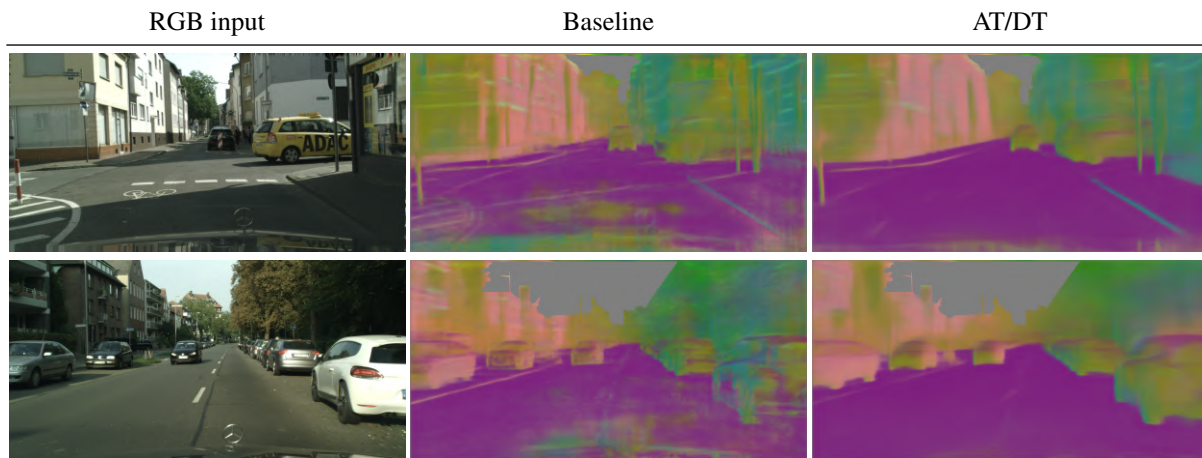


Figure 4: Qualitative results on Cityscapes dataset in a *Sem.*  $\rightarrow$  *Norm.* scenario. From left to right: RGB input, prediction obtained by a transfer learning baseline and by our framework (AT/DT).

we define as the set of points at infinite depth. To evaluate the trained network on Cityscapes we collapse some of the available classes to make them compatible with Carla: *car* and *bicycle* collapse into *vehicle* and *traffic sign* and *traffic light* into *traffic sign*. We ignore the other labels of Cityscapes which do not have a correspondent class in Carla.

**Depth** We trained and evaluate the depth networks clipping the max predictable depth to 100m and then normalizing between 0 and 1. At inference time we scale the predictions back to the 0m-100m range before computing the different metrics.

## References

- [1] D. P. Kingma and J. Ba. Adam: A method for stochastic optimization. In *ICLR*, 2015. 3
- [2] P. Z. Ramirez, M. Poggi, F. Tosi, S. Mattoccia, and L. Di Stefano. Geometry meets semantics for semi-supervised monocular depth estimation. *arXiv preprint arXiv:1810.04093*, 2018. 1
- [3] L. van der Maaten and G. Hinton. Visualizing data using t-SNE. *Journal of Machine Learning Research*, 9:2579–2605, 2008. 2, 3
- [4] F. Yu, V. Koltun, and T. Funkhouser. Dilated residual networks. In *Computer Vision and Pattern Recognition (CVPR)*, 2017. 2
- [5] J.-Y. Zhu, T. Park, P. Isola, and A. A. Efros. Unpaired image-to-image translation using cycle-consistent adversarial networks. In *The IEEE International Conference on Computer Vision (ICCV)*, Oct 2017. 2, 4